

# Superconducting nanowires connected in series for photon number resolving functionality.

F. Mattioli<sup>1</sup>, S. Jahanmirinejad<sup>2</sup>, Z. Zhou<sup>2</sup>, A. Gaggero<sup>1</sup>, G. Frucci<sup>2</sup>, D. Sahin<sup>2</sup>, R. Leoni<sup>1</sup>, and A. Fiore<sup>2</sup>

<sup>1</sup> Istituto di Fotonica e Nanotecnologie, CNR, Via Cineto Romano 42, 00156 Roma, Italy

<sup>2</sup> COBRA Research Institute, Eindhoven University of Technology, PO Box 513, 5600 MB Eindhoven, The Netherlands

Francesco.mattioli@ifn.cnr.it

**Abstract.** The experimental demonstration of a superconducting photon-number-resolving detector, based on the series connection of  $N$  superconducting nanowires, is presented. An integrated resistor is connected in parallel to each section of the device that provides in this way a single voltage-readout, proportional to the number of photons detected in distinct nanowires. As a proof of principle a four element detector has been fabricated from an NbN film on a GaAs substrate and fully characterized. Clearly separated output levels corresponding to the detection of  $n = 1 - 4$  photons are observed achieving a single-photon system quantum efficiency of 2.6% at  $\lambda=1.3 \mu\text{m}$ . In order to demonstrate the potential scalability of the series-nanowire detector to a larger number of photons, we report our preliminary results in the characterization of detectors fabricated with 8 and 12 pixels. Clear evidence of  $n=1-8$  photon absorption in the 8-pixel detector has been achieved.

## 1. Introduction

Single-photon detection needs highly sensitive devices, which, for this reason, operate in a strongly nonlinear mode. Their response in this regime is independent from the number of detected photons. On the contrary, conventional optical detectors generate an electrical signal that is proportional to the intensity of the incident light, but their sensitivity is strongly limited by the electrical noise in the circuit needed for the signal amplification. In the last years, great efforts have been devoted to fill the gap between those two distinct regimes, creating a device capable of determining the number of incident photons: a photon-number-resolving (PNR) detector. Even though several detector technologies combining linear operation and single-photon sensitivity have been proposed, in the telecommunication wavelength region, which is interesting for many applications, their performance has remained limited in terms of speed and dynamic range. Transition-edge-sensors operating at sub-Kelvin temperatures show relatively slow response times [1]. Self-differencing InGaAs avalanche photodiodes (APDs) offer limited photon number discrimination ability [2]. APDs have been time-multiplexed to achieve photon number resolving capability, but with a necessarily reduced count rate due to the delay loops [3, 4]. The silicon photomultiplier (SiPM) combined with frequency up-conversion provides PNR functionality with large dynamic range, but introduces added noise due to



the up-conversion process and cross-talk between the pixels [5]. In this framework it is natural to take advantage of the very high sensitivity, short dead time, and low timing jitter of SSPDs in the near-infrared range [6]. While multi-element SSPD arrays with separate readout for each element have been proposed [7], a configuration with a single readout is preferable in terms of simplicity and scalability to large photon numbers. Indeed, exploiting new geometries and using the spatial multiplexing it is possible to achieve a photon number resolving capability with SSPDs. For this reason in the past a parallel configuration with single output (parallel nanowire photon-number-resolving detector, PND) [8] has been proposed. However, this configuration has a limited dynamic range and efficiency, due to the current redistribution issue that increases the bias current in the unfiring sections, potentially leading to spurious switching [9].

In this article, we describe recent results on the photon-number-resolving detector based on the series connection of nanowires (series-nanowire detector, SND), theoretically proposed in Ref. [10]. A 4-pixel proof-of-principle detector was already characterized in Ref. [11]. Here, to demonstrate the scalability to large photon numbers of the series-nanowire structure, we present results on 8- and 12-pixels devices. The results on an 8-pixel SND show clear evidence of detection of  $n$ -photons with  $n$  ranging from 1 to 8.

## 2. Design and sample fabrication

### 2.1. Design

The electrical structure of the SND is based on the series connection of several wires, each shunted by a resistance (see figure 1) [10]. As in standard SSPDs, the nanowire is biased with a current close to its critical current ( $I_C$ ), and after a single photon is absorbed, a resistive region is formed across the nanowire [6]. Due to the presence of the resistances integrated in parallel to each meander section (figure 1), the bias current ( $I_b$ ) flows into these resistances rather than into the external load, producing a voltage pulse. If several sections switch simultaneously, the bias current flows into several parallel resistances, giving rise to a voltage across the whole device proportional to the number of switching sections [10].

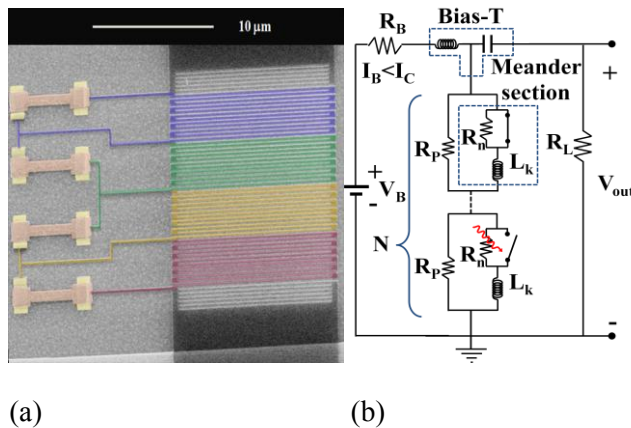


**Figure 1.** (a) SEM image of the 4-pixel SND where the active wires, the parallel resistors, and their contact pads have been colored for clarity. (b) Equivalent electrical circuit of an  $N$ -element SND structure in which the last section has absorbed a photon. Each meander section is represented as a switch in parallel with the nanowire normal resistance and then in series with its kinetic inductance (the switch is closed in the superconducting state and opens when a photon is absorbed).

This device is designed as the electrical dual of the parallel nanowire photon-number-resolving detector in order to solve the current redistribution problem. All the detecting sections are biased with the same bias current ( $I_B$ ) close to the critical one ( $I_C$ ) (figure 1(b)). Switching of a wire in the SND reduces the bias current in the other unfiring wires (because a part is also diverted into the external load), as compared to the PND where the current in the unfiring wires is increased [9]. In this way, the SND can be biased closer to the critical current reaching higher quantum efficiency and more sections can be added in series allowing scaling to large photon numbers. In terms of response amplitude and speed, the device performance can be further optimized using a cryogen high-impedance preamplifier stage (high electron mobility transistor mounted close to the SND).

## 2.2. Fabrication process for 4-, 8- and 12-pixel SNDs

The SNDs are fabricated starting with 4.5nm, 4.8nm and 4.8nm thick NbN film (for the 4-SND, 8-SND and 12-SND, respectively) grown on GaAs substrates by reactive magnetron sputtering, at 410°C. The film parameters are a superconducting transition temperature of 9.5K and a transition width of 0.7K. Four steps of direct-writing electron beam lithography (EBL) are used to define the geometry of the SPD. For electron beam lithography a high resolution Vistec EBP5 5HR is used: this system is equipped with a field emission gun with 100 kV acceleration voltage. In the first step, Ti(10nm)/Au(60nm) electrical contact pads are patterned as a 50  $\Omega$  coplanar transmission line, together with alignment markers, using a positive tone PMMA electronic resist, followed by metal evaporation and lift-off. To obtain the electrical contact between the nanowires and the parallel resistances, additional Ti(5nm)/Au(200nm) pads are needed and are defined in a second step (light yellow-coloured pads in figure 1(a)). In the third step a 140 nm thick hydrogen silsesquioxane (HSQ) mask is used to define the 100 nm wide meandered nanowires, covering a total active area of 12 x 12  $\mu\text{m}^2$  with a 40% filling factor. Great care has been devoted to this lithographic step: in order to obtain a uniform width of the nanowire, during the e-beam exposure of the meander we varied locally the electronic dose reducing it towards the centre of the pattern. The pattern obtained in this way on the HSQ mask, is then transferred onto the NbN film underneath with a reactive ion etching (RIE) process based on a  $\text{CHF}_3$ ,  $\text{SF}_6$  and Ar mixture. The fourth step is used for the Ti (10 nm)/AuPd (50 nm) resistances definition. Each of them is 500 nm wide and 3.5  $\mu\text{m}$  long corresponding to a design value of  $R_p = 50\Omega$ . The fabricated structures are shown in the scanning electron microscope (SEM) image in figure 1 (a) and figure 2.

## 3. Optical characterization

The electro-optical characterization of the SND has been obtained in a closed-cycle cryocooler with a base temperature of 1.2K. The bias current is supplied through the DC port of a bias-T by a voltage source in series with a 10 $\Omega$  bias resistor: the IV curve of this device is different from the standard SSPD IV curves due to the presence of the parallel resistance.

A pulsed laser-diode (50 ps pulse width, 1.3  $\mu\text{m}$  wavelength, and 10 MHz repetition rate) has been used for the optical characterization. The coupling to the device has been achieved by means of a single-mode polarization maintaining lensed fiber, mounted on a XYZ piezo stage for the alignment. The beam has been defocused to a spot diameter of about 20  $\mu\text{m}$  in order to illuminate equally all sections of the SND (12 x 12  $\mu\text{m}^2$  active area). A 40-GHz bandwidth sampling oscilloscope or a 350 MHz counter have been used for optical characterization to analyze the output signal collected at room temperature through the RF arm of the bias-T and amplified using a chain of wideband amplifiers.

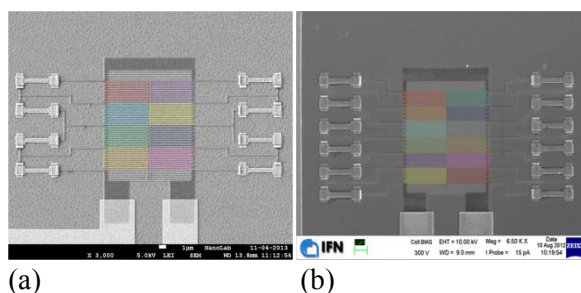


**Figure 2.** (a) SEM image of the fabricated 8-SND with pixel colored with different colors. (b) SEM image of the 12-SND with pixel colored with different colors.

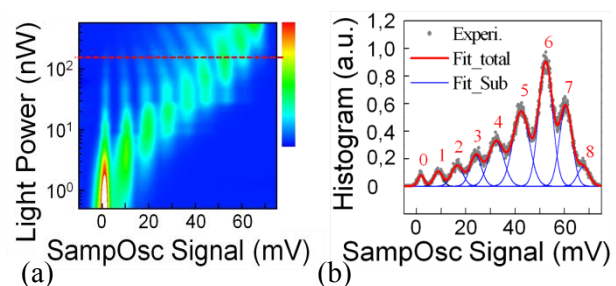


**Figure 3.** (a) Counts as a function of voltage and light power taken with  $\lambda = 1.3 \mu\text{m}$  and 14 MHz repetition rate (b) Histogram (gray line) at the light power indicated as a red dashed line in figure 3 (a), showing 8 clearly spaced peaks, and fit (red line), assuming each photon level contributes a Gaussian voltage distribution (blue lines)

### 3.1. 4-pixel SND

Results of 4-pixel SNDs were already reported in ref. [11]. Four clear peaks have been observed and it has been proved that they correspond to the detection of 1–4 photons. The highest value of the single-photon system quantum efficiency (SQE) was 2.6% (with the spot focused on the device) at a bias current of  $I_B=12.4 \mu\text{A}$  ( $0.99 I_C$ ), with the light polarized parallel to the wires. The capability of biasing the device at 99% of the  $I_C$  demonstrates the correct functionality of the series nanowire configuration. At low bias currents ( $I_B < 10 \mu\text{A}$ ) a dark count rate (DCR) as low as 1 Hz is measured. At  $I_B=10 \mu\text{A}$ , a SQE of 1% and a DCR of 5Hz are obtained. The approaches used to increase the quantum efficiency of SSPDs can also be applied to SNDs: Improvement of the superconducting properties of the thin film [12, 13], reduction of the width of the nanowires [14] and implementation of advanced optical cavities [15-17] or waveguides [18].

### 3.2. 8-pixel SND

The fabrication process already described and a similar optical characterization has been applied to SNDs with 8 and 12 pixels, shown in figure 2 (a) and (b), respectively. Figure 3 shows clear evidence that  $n=1-8$  detection events have been observed in the 8-pixel SND. Figure 3 (a) shows the color plot of the counts as a function of the pulse height voltage taken for different attenuations of the laser pulse: the pulse height distribution taken for a particular light attenuation (red dashed line in figure 3 (a)) is showed in figure 3(b). All the eight peaks are clearly visible (every peak is separated from the others) and evenly spaced. A full optical characterization of this 8-SND together with the first tests on the 12-SND are in progress.

## 4. Conclusions

In conclusion, a design for PNR detectors based on the series connection of  $N$  superconducting nanowires sections, each shunted with a resistance, has been described and implemented. The detection of  $n=1-4$  photons in the telecom wavelength range has been demonstrated in a 4-pixel SND with maximum system quantum efficiency of 2.6% and recovery time constant in the 10 ns range. The integration of the SND with an optical cavity will lead to the improvement of the SQE. Scaling to large number of sections has been realized up to 12 element detector, keeping the same active area of the device. Clear evidence of the detection of  $n=1-8$  in the 8-pixel SND has also been reported.

## References

- [1] Lita A E, Miller A J and Nam S W 2008 *Opt. Express* **16**(5) 303.
- [2] Kardynal B E, Yuan Z L and Shields A J 2008 *Nat. Photonics* **2** 425.
- [3] Fitch M J, Jacobs B C, Pittman T B and Franson J D 2003 *Phys. Rev. A* **68** 043814.
- [4] Eraerds P et al. 2010 *Rev. Sci. Instrum.* **81** 103105.
- [5] Pomarico E, Sanguinetti B, Thew R and Zbinden H 2010 *Opt. Express* **18**(10) 10750.
- [6] Gol'tsman G et al. 2001 *Appl. Phys. Lett.* **79** 705.
- [7] Dauler E A et al. 2009 *J. Mod. Opt.* **56** 364.
- [8] Divochiy A et al. 2008 *Nat. Photonics* **2** 302–306.
- [9] Marsili F, et al. 2009 *New J. Phys.* **11** 045022.
- [10] Jahanmirnejad S and Fiore A 2012 *Opt. Express* **20** 5017.
- [11] Jahanmirnejad S et al. 2012 *Appl. Phys. Lett.* **101** 072602.
- [12] Tanner M G et al. 2010 *Appl. Phys. Lett.* **96** 221109.
- [13] Baek B, Lita A E, Verma V, and Nam S W 2011 *Appl. Phys. Lett.* **98** 251105.
- [14] Marsili Fet all. 2011 *Nano Lett.* **11**(5) 2048–2053.
- [15] Gaggero A et al. 2010 *Appl. Phys. Lett.* **97** 151108.
- [16] Rosfjord K M et al. 2006 *Opt. Express* **14** (2) 527–534.
- [17] Baek B, Stern J A, and Nam S W 2009 *Appl. Phys. Lett.* **95** 191110.
- [18] Sprengers J Pet all. 2011 *Appl. Phys. Lett.* **99** 181110.